CHAPTER II

THEORY

2.1 Zeolites

Zeolites are microporous crystalline aluminosilicates that has been studied by mineralogist for more than 200 years. They are comprised of channel and cavities of molecular dimensions ranging from 3 to 10 Å on diameter. The general formula for the composition of zeolite in the hydrated form is:

$$M_{x/n}\,[(AlO_2)_x(SiO_2)_y].\ w\ H_2O$$

Where M is an extra framework cation that balances the anionic charge of the framework, n is the cation valence for M, x and y are the total number of aluminates and silicates per unit cell and z is the number of water molecules per unit cell. Typical cation include alkali metals, e.g. Na^+, K^+, alkaline earth metals, e.g. Ca^{2+}, Ba^{2+} and other cation such as NH_4^+ and H^+ [51].

The application area of natural zeolite can be broadly classified as building materials, agriculture, ion exchange, adsorbent and others. The adsorption and ion exchange properties of natural zeolites are exploited in application such as odor removal, fertilizer acid, soil amendment, animal feed supplement, water treatment, aquaculture, removal of radioactive species and heavy metals from waste streams, heat storage and solar refrigeration, pollution control and miscellaneous other used.

With the great demand of zeolites for commercial applications, zeolites are produced synthetically in large industrial quantities. More than 150 zeolite have been synthesized. Synthetic zeolites were first prepared in the 1950s by the Union Carbide Corporation USA. The sereral typed of zeolites were synthesized commercially such as zeolite A, X, Y, mordenite and ZSM-5. Zeolite Y was used as an isomerization atalyst and zeolite X was used as a cracking catalyst in petrochemical process in 1959 and 1962, respectively [52].

All the synthetic zeolite are distinguishable from each other and from natural zeolites on the basis of composition, crystal structure and sorption properties. The

properties of synthetic zeolite that are exploited commercially are adsorption, catalytic activity and ion exchange. Catalysis is a major area of usage for the synthetic zeolites (Figure 2.1). Several catalysts developed during the 1960s have virtually revolutionized the refining of oil to gasoline and other products. Molecular sieving and shape selectivity became possible with the synthetic catalysts. Shape selective catalysis can be performed inside the zeolite's cavities to give a single product [51]

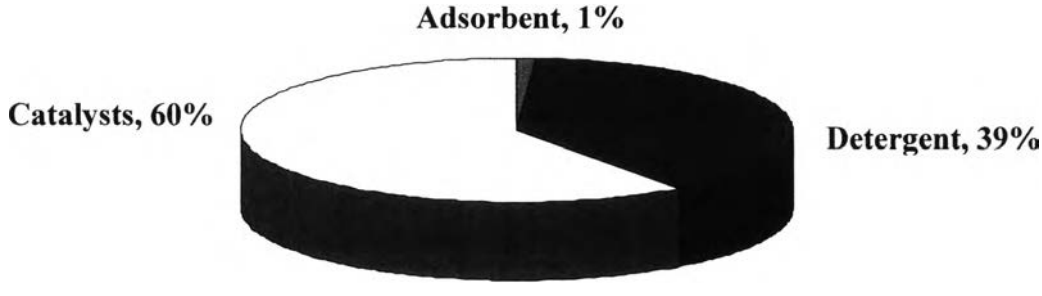

Figure 2.1 Zeolite utilization in united state of American in 1995.

The earliest application of zeolite selective catalysis is the alkylation of toluene to give exclusively para-xylene, the key intermediate for a number of polymers. Apart from toluene disproportionation, processes using shape-selective zeolite catalysts are mostly in the petroleum and petrochemical industries such as benzene alkylation, xylene isomerization, catalytic cracking and conversion of methanol to gasoline. The successes of these catalytic applications have assured a bright future for research on zeolite material [52].

2.1.1 Zeolite Structures

Zeolite structures are composed of an infinitely extending three dimensional network of SiO_4 and AlO_4 tetrahedra. The tetrahedra are cross linked by the sharing of oxygen ions resulting in the empirical formula of $[SiO_2]$ and $[AlO_2]^-$ [53]. These tetrahedra refers to Primary Building Units (PBU) (Figure 2.2), and then the PBUs are assembled into Secondary Building Units (SBUs) (Figure 2.3), which are themselves assembled to form the zeolite structure framework. The PBUs of

zeolite structure is a tetrahedral unit is composed of a central Si or Al atom surrounded by four oxygen atoms, namely $[SiO_2]$ or $[AlO_2]^-$ [54]. These tetrahedrals are linked through the oxygen atoms to form channels and cages of discrete size with no two aluminum atoms can share the same oxygen.

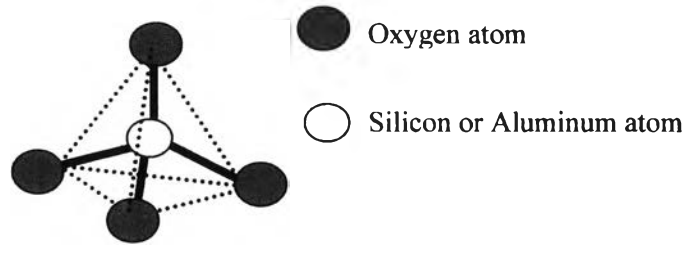

Figure 2.2 A primary building unit (PBU) : $[SiO_2]$ or $[AlO_2]^-$

As a result of the negative charge from the framework charge of zeolite is negative and hence must be balanced by cations, typically from the alkali or alkaline earth metal cations. These cations can be exchanged by various types of cations, particulariy +1 to +3 species. The position, size and number of cations can significantly alter the properties of zeolites. Figure 2.4 depicts schematically the buildings of zeolite framework [55]. Several tetrahedral units are joined so that each of four oxygen atoms is shared with another tetrahedral silica or alumina to form a wide range of small SBUs, as shown in Figure 2.4b. These SBUs are interconnected to produce a wide range of tertiary building units or polyhedra which in turn are arranged in a three dimensional pattern to form extended characteristic framework of various zeolite crystal structures (Figure 2.4c). In these structures the corners of polyhedra represent Si or Al atoms and the connecting line are the distance between the centers of neighboring tetrahedral units while oxygen atoms an omitted for the ease of structure demonstrated.

Zeolite pore consist of 8, 10 and 12 membered oxygen ring systems to form channels and pores which is interrelated to each other on zeolite framework. The channels may one, two or three dimension with different sizes. Zeolites can be classified according to their diameter of pore size (ϕ); small pore which consist of 8-membered of oxygen ring systems with $\phi < 4$ Å such as zeolite A, chabazite and

erionite; mrdium pore zeolite which concists of 10-membered of oxygen ring systems within 4.5 Å < ϕ< 6.5 Å such as ZSM-5, ferierite and TS-1 and large pore zeolite with 12-membered oxygen ring systems with ϕ > 6.5 Å such as mordenite, faujasite and zeolite beta [53]. Pore size of zeolite is around 3.5 Å to 8.0 Å which can separate the selective organic molecules based on their sizes.

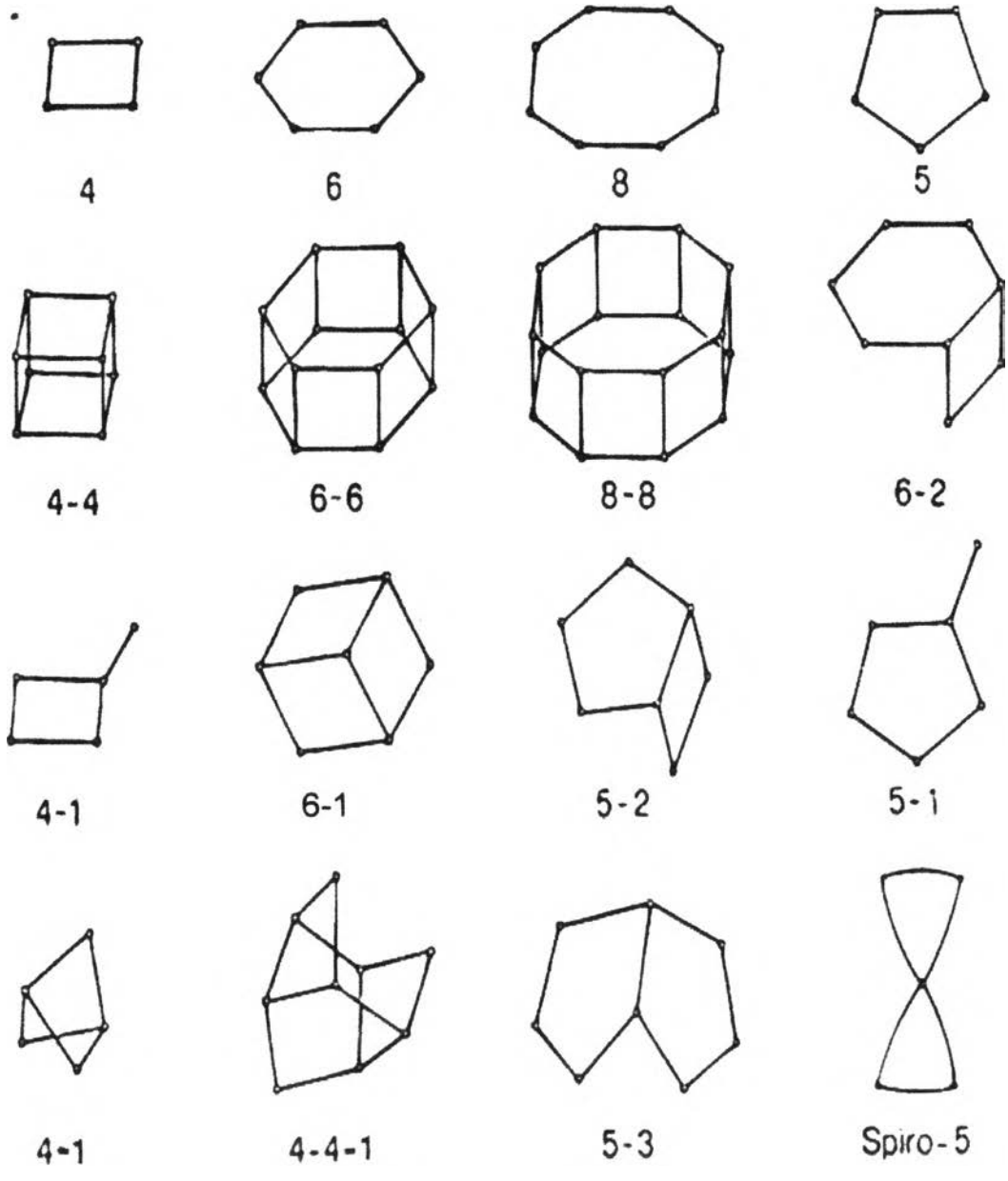

Figure 2.3 The secondary building units (SBU) found in zeolite framework [56]

\

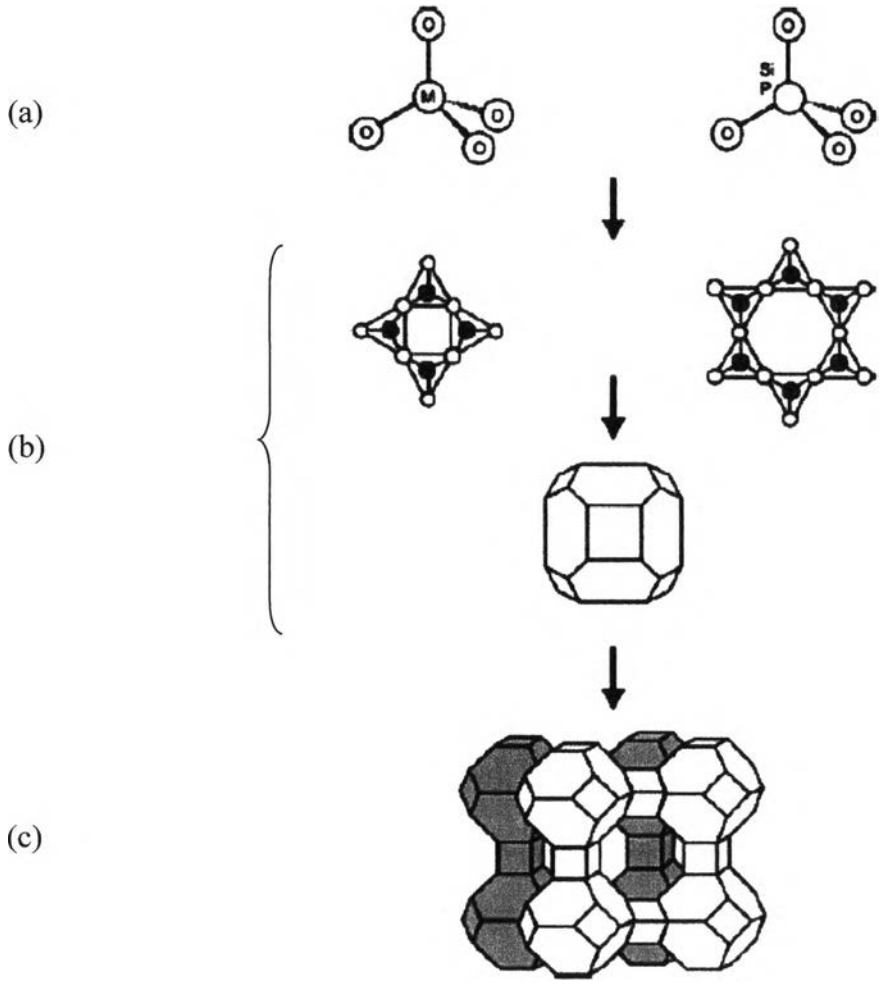

Figure 2.4 Schematic representative of the building of zeolite framework [56]
(a) Primary building units (b) Secondary building units and
(c) Structure of zeolite A

2.1.2 Acidity of Zeolites

Acidity is one of the most important characteristics of zeolites and is very useful in acid catalysis. A good understanding of the nature and number of acid sites in a zeolite in needed in developing improved and novel catalysts for applications in the chemical industries [57]. The activity of zeolites as acid catalysts is related to the acidity of active sites on their surface [58].

The framework aluminum atoms are negatively charged and balanced by extra-framework cations, represent potential active acid site it the cations are H^+ [54]. The acidic properties of zeolites are mainly dependent on the Si/Al molar ratio as well as the temperature of activation. In zeolites, acid sites are classified according to the classical Brønsted and Lewis acid models (Figure 2.5). Brønsted acid corresponds to proton donor, while Lewis acid corresponds to electron pair acceptor. Brønsted acid occurs when the cations used for balancing the negatively charged framework are proton (H^+). A trigonally coordinated aluminum atom possessing a vacant orbital that can accept an electron pair, behaves like a Lewis acid site.

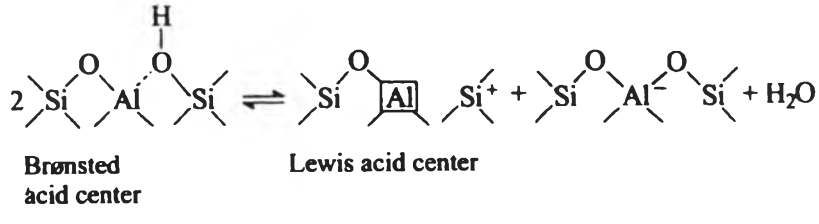

Figure 2.5 Brønsted and Lewis acid site in zeolites

In the majority of the as-synthesized commercial zeolites, the cation is sodium ions (Na^+) and the corresponding zeolite is referred to the sodium form (Figure 2.6a). To obtain the acid form of zeolites, Na^+ are replaced by protons via ion-exchange with an aluminum salt (Figure 2.6b), followed by calcination at high temperature to decompose NH_4^+ ions into H^+ and NH_3 (Figure 2.6c). After the liberation of ammonia, protons are bonded with surface oxygen to give the bridging form -SiO(H)Al- of Brønsted acid sites. An equilibrium exists between this bridging form and the other form in which silanol (-SiOH) group is adjacent to a tricoordinate aluminium that constitutes the Lewis acid site (Figure 2.6 d). A further increase in

calcination temperature (>500°C) in the presence of steam results in the dehydroxylation process where Brønsted acid sites are converted to Lewis acid sites.

The catalytic activity of proton-exchange zeolite is also determined by the strength of the acid. In general, the lower of aluminium content of a zeolite or the higher the Si/Al ratio, the stronger the Brønsted acidity is several characterization techniques have been developed to qualitatively and quantitatively estimate the acid sites and the relation between catalytic behavior of zeolite and their acidity. The most widely used techniques are temperature programmed desorption (TPD) of ammonia, FTIR spectroscopy and a catalytic testing in reaction [59].

The temperature programmed desorption of adsorbed NH_3 molecules is used for determination the amount and strength of acid sites. Ammonia is the preferred adsorbing or desorbing gas because of its small size (kinetic diameter, 2.62 Å) and its weak basicity ($pK_b = 4.75$). It can reach practically all the acid sites at the given temperature. Upon desorption at rising programmed temperatures, NH_3 molecules will gradually desorp from the acid sites. The latter aspect is followed up of the amount of NH_3 desorption plotted against the temperature.

FTIR spectroscopy has been also applied extensively to study the nature and the amount of acid sites present in zeolite. Infrared spectroscopy (IR) has proven to be a valuable tool in characterizing hydroxyl species on the surface of molecular sieves and in measuring Brønsted and Lewis acidity [60]. IR studies of zeolite Beta have revealed two hydroxyl stretching bands, one at approximately 3605 cm^{-1} and another at approximately 3740 cm^{-1}. The band at 3605 cm^{-1} has been identified as the hydroxyl stretch associated with the bridging Al-O(H)-Si [61-63].

The band at 3740 cm^{-1} has been attributed to the terminal silanol Si-OH groups on the external crystal surface. Weak bases such as pyridine and ammonia have been widely used as probe molecules in adsorption or desorption studies for the determination of Brønsted and Lewis acidity by IR spectroscopy. A stretching vibration at 1545 cm^{-1} is attributed to the pyridinium ion, i.e. the Brønsted-bound pyridine, whereas the stretching vibration at 1450 cm^{-1} is attributed to the coordinated pyridine to extra framework aluminium and well known as Lewis acid site [61]. A combination band or overlapping band at 1490 cm^{-1} is due to both Lewis and Brønsted bound pyridine stretching vibration and band at 1620 cm^{-1} due to Lewis bound pyridine.

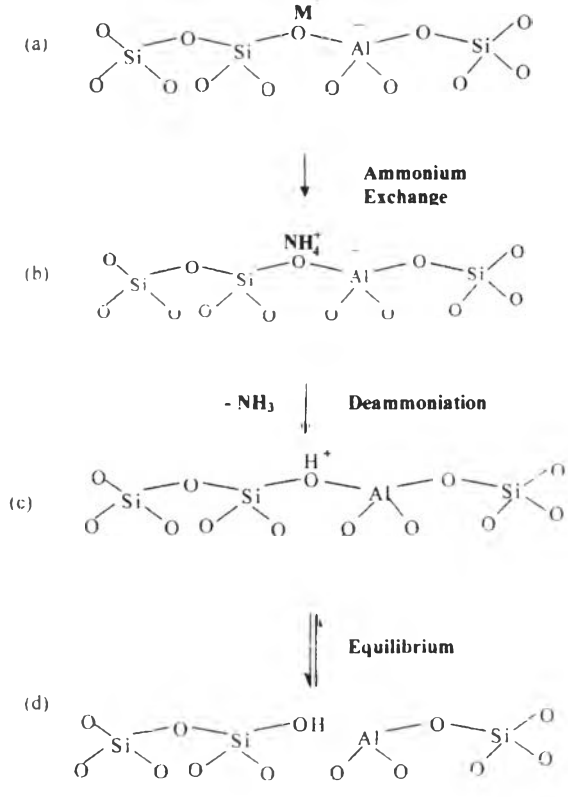

Figure 2.6 Diagram of zeolite framework surface (a) In the as-synthesized form, M^+ is either an organic cation or an alkali metal cation. (b) Ammonium ion exchange produces the NH_4^+ exchanged form. (c) Thermal treatment is used for removal of ammonia, producing the H^+, acid form. (d) Equilibrium form showing a silanol group adjacent to a tricoordinate aluminium.

2.1.3 Shape and Size Selectivity

Shape and size selectivity plays a very important role in catalysis. Highly crystalline and ordered channel structures are among the principal features that zeolites used as catalysts offer over other materials. Shape selectivity is divided into 3 types: reactant shape selectivity, product shape selectivity and transition-state shape selectivity. They are illustrated in Figure 2.7. Reactant shape selectivity results from the limited diffusivity of some reactants, which cannot effectively enter and diffuse inside the zeolites. Product shape selectivity occurs when diffusing product molecules cannot rapidly escape from the zeolite pore and undergo further reactions. Restricted transition-state shape selectivity is a kinetic effect arising from the local environment around the active site: the rate constant for a certain reaction mechanism is reduced if the necessary transition state is too bulky to form readily.

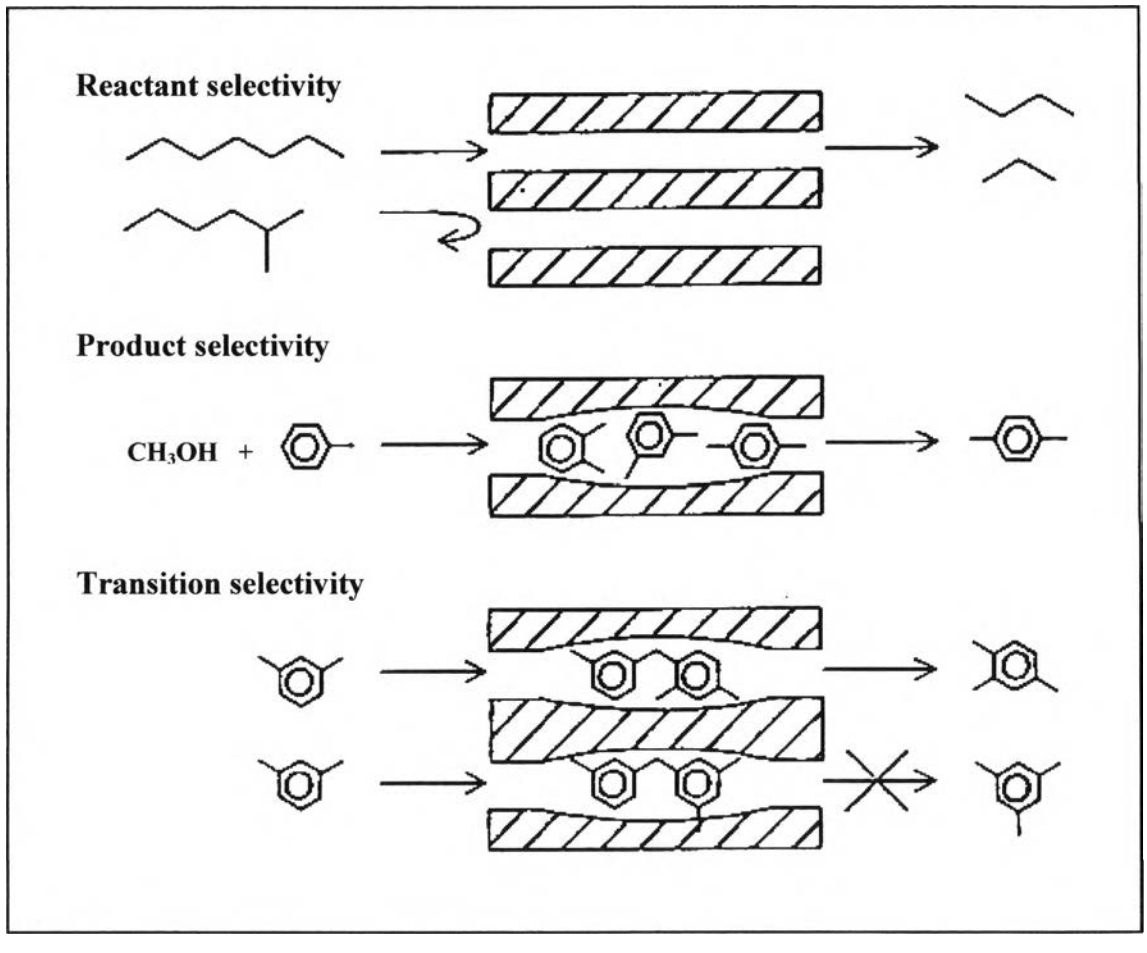

Figure 2.7 Three types of selectivity in zeolites: reactant, product and transition-state shape selectivity. [60]

2.1.4 Synthesis of Zeolites

Zeolites form in nature or in the laboratory at elevated temperatures and under hydrothermal conditions [54]. In zeolite synthesis, the reaction mixture is composed of the main reactants which are silica, alumina, sodium hydroxide and water with the amounts corresponding to the composition of the desired product. The reaction maintained for a period of time at constant pressure and temperature. The usual sources of aluminium are aluminium hydroxide or sodium aluminate, while amorphous silica, sodium silicate, sodium metasilicate, silica glass, silicilic acid and various concentrations of silica sol are the common silica sources used in zeolite synthesis and they are available commercially. Beside the commercial silica, the uses of high silica content of low cost and waste materials such as fly ash and rice husk ash as a silica sources are desirable. Rice husk ash is already known as a silica sources for synthesizing zeolite Beta [36], zeolite Y [64], ZSM-5 [65] and mordenite [66]. The conditions for preparation zeolites depend on the type of zeolites that one needs to synthesize. The reaction mixture and the synthesis condition are different depending on the type of zeolites, and the silica content in the product, *i.e.* low silica zeolite (Si/Al < 5) or a high silica zeolite (Si/Al > 5). The temperature to prepare high silica zeolites is generally higher than that for low silica zeolites. Besides, the synthesis of high silica zeolites requires the addition of templates, which are alkylammonium cations. Templates and silica were used in considerable amounts as reactants in zeolite synthesis compared to other reactants. Many types of organic templates are regularly used in the synthesize of zeolites with high silica content such as tetraethylammonium hydroxide (TEAOH), tetrapropylammonium hydroxide, tetraethylammonium halide [67] and etc. One type of template can be used for crystallize various types of zeolites whereas the same type of zeolite may be formed by using different templates. For example tetraethylammonium hydroxide was used as an organic template in the synthesis of zeolite Beta, mordenite and ZSM-20. Zeolite Beta can also be synthesized by using tetraethylammonium bromide as an organic template. The template is functioned as the structure directing agent while organic or inorganic compounds functioned as the cations to neutralize the anionic framework charge. This template is removed by calcination to obtain the porous structure. The zeolite formed is determined by the synthesis parameter such as alkalinity, temperature, crystallization period and gel ratio of the reactants. The alkalinity is

related to the total sum of tetrahedron $[Si(OH)_4]$ and $[Al(OH)_4]^-$ concentrations, which are functioned as structure builder of zeolite framework. The optimum condition for zeolite synthesis is in the region of pH 11 to 13 which is suitable for zeolite crystallization. Temperature is a thermodynamic factor which influences the rates of nucleation, crystal growth, crystal types and crystal size which will be formed. At certain temperature, certain crystal will be formed. For example, a gel mixture produced crystal of analcime when hydrothermal synthesis wasried out at 150°C, although at 110°C the mixture of analcime and gismondine was formed. At lower temperature; 80°C only gismondine crystal was formed [53]. The crystallization period also influences nucleation and crystal growth. The crystallization period decreases rapidly with increasing temperature. At the same temperature, different phases of zeolites will be formed depending on the crystallization period. For example at 170°C, ZSM-48 and ZSM-39 were formed in the synthesis reported by Suzuki and Hayakawa [68]. All components in the initial reaction mixture play their own role on influencing the crystallization of zeolite. The type of silica phase will determine the rate of solubility of the silica. For example, amorphous silica dissolves faster than crystalline silica. The ratio of gel mixture also influences the nucleation, crystal growth and type of zeolites formed. For example, the synthesis of zeolite at SiO_2/Al_2O_3 of 10 in initial gel will produce analcime and mordenite while zeolite beta was formed at SiO_2/Al_2O_3 of 15 in initial gel, while the rest of the reactants were kept constant. Another factor in zeolite crystallization is the concentration of hydroxyl ion which is provided by sodium hydroxide. The high concentration of hydroxyl ion increases the alkalinity of the solution and the crystalline phase obtained might differ from the lower concentration of hydroxyl. Alkaline solution will facilitate the solubility of silica which increases the crystallization rate. At higher ratio SiO_2/Al_2O_3, hydroxyl ion will produce unstable solution due to the lack of charge compensation. For example, at a fixed SiO_2/Al_2O_3 ratio and at a constant time of crystallization, increase of hydroxyl ion favors the formation of mordenite over ZSM-5 [69].

Hydrothermal syntheses of silica-rich zeolites generally consist of water as the solvent, a silicon source, an aluminum source, and a structure-directing agent. Better understanding of the effect of the structure-directing agent has long been aimed at. This will entail better control of the resulting structures, and even prediction of the specific structure could be possible. Some progress in the field has been made some

general rules of correlation between the structure-directing agent and the structure of zeolites with high silica content:

1. Hydrothermal silicate syntheses result in dense crystalline and layered materials when no structure-directing agent is present.
2. Linear structure-directing agents usually result in one-dimensional molecular sieves with 10-ring channels.
3. Branched structure-directing agents tend to form multi-dimensional zeolites with pore diameters of 4-7 Å.
4. One-dimensional, large pore zeolites often result from large polycyclic structure-directing agents.

2.2 Zeolite Beta

Zeolite beta was first synthesized by Wadlinger, Kerr and Rosinski in 1967 [24]. Zeolite beta represents the first high silica zeolite (Si/Al = 10-100) synthesized from a gel with alkali metal and organic template, tetraethylammonium cation. It can be described by the general formula:

$$Na_n[Al_nSi_{64-n}O_{128}], \text{ where } n = 7$$

The structure of zeolite beta was described by Treacy et al.[70] and Higgins *et al.*[71]. The first clues to the crystal structure of zeolite beta were evident from chemical and physical property measurements. Ion-exchanged isotherms of Na-Beta at 25°C indicated that cations as large as tetraethylammonium ion, (TEA^+) exchange completely into the pore system. This behavior suggests that zeolite beta contains at least 12 membered rings opening into channel, because TEA^+ is too large to be exchanged through 10 membered-rings such as those in ZSM-5. The complete exchanged of cations in zeolite beta indicated the presence of channels instead of cages, because it is not possible to remove all the cations from the cage structures as found in the cage structure of Na faujasite.

Zeolit beta in an intergrowth hybrid of two distinct but closely related structures [72] which have tetragonal and monoclinic symmetry. In both systems, straight 12 membered-ring channels are present in two crystallographic directions perpendicular to [001] (Figure 2.7), while the 12 membered-ring in the third direction, parallel to the

c axis, is sinusoidal. The sinusoidal channels have circular openings (5.6 Å), and the straight channels have elliptical openings (Figure 2.8). The only difference between the two polymorphs (polymorphs A and B) is in the pore dimension of the straight channels. In the tetragonal system, the straight channels have openings of 6.0 x 7.3 Å, whereas in the monoclinic system they are 6.8 x 7.3 Å (Figure 2.8). A third polymorph, named C, has recently been suggested by Higgens, *et al.*[71], also having monoclinic symmetry. Figure 2.11 shows zeolite beta framework viewed along [100] and [001]. Figures 2.9 and 2.10 show channel system in zeolite beta structure. The three type of polymorphs of zeolite beta are shown in Figure 2.11.

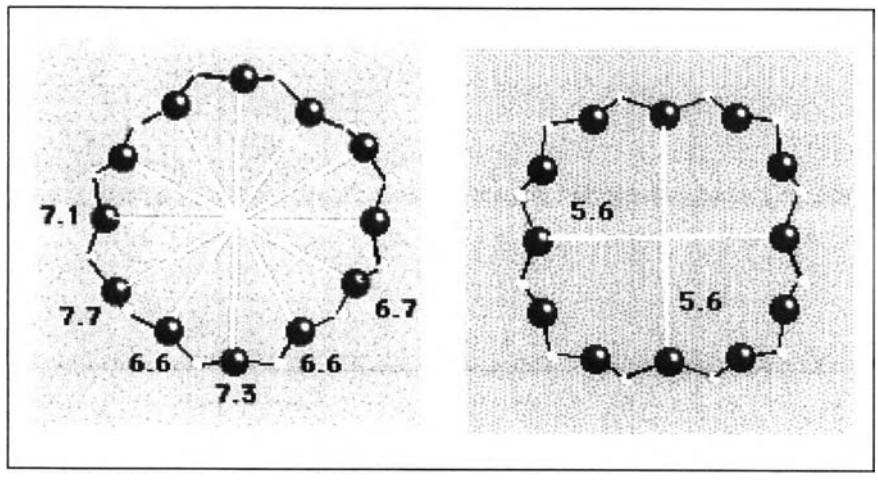

Figure 2.8 Zeolite beta framework viewed along (a) [100] and (b) [001]

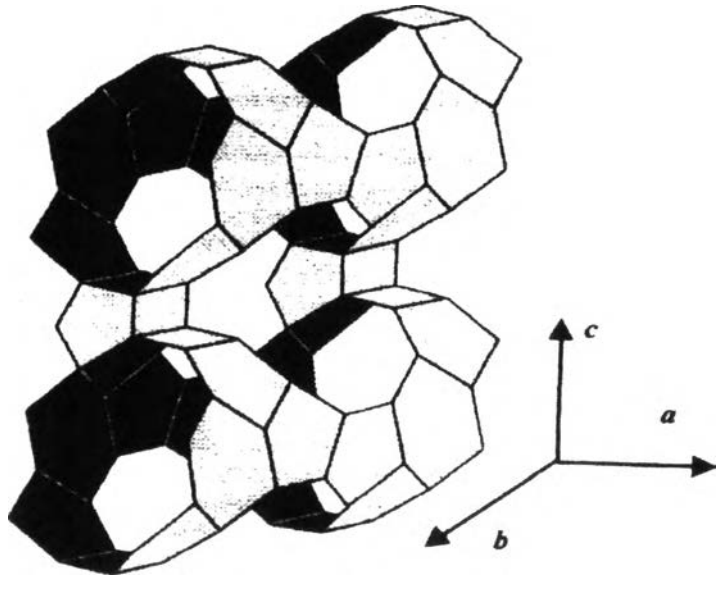

Figure 2.9 Three-dimensional structure of zeolite beta

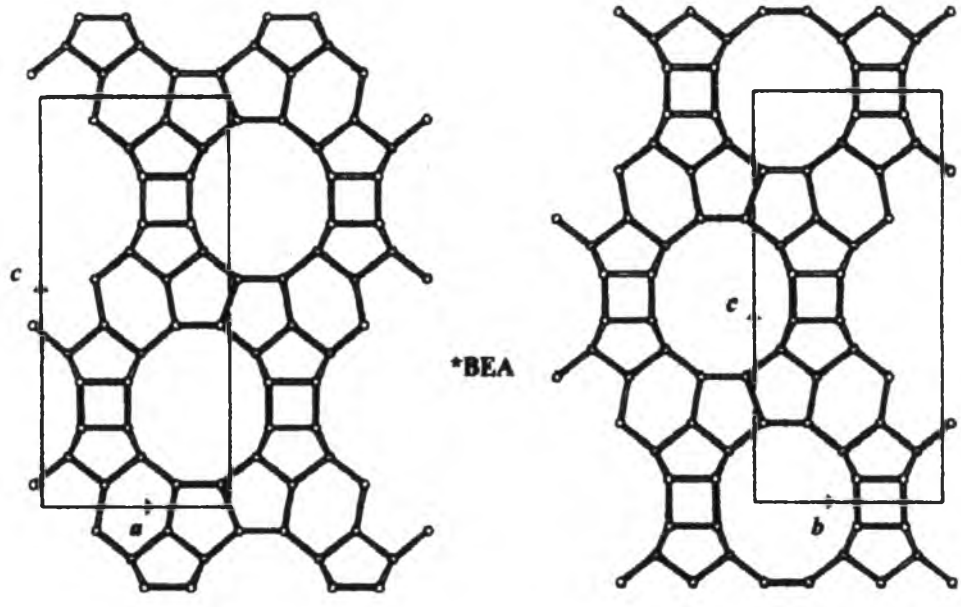

Figure 2.10 Zeolite beta structure

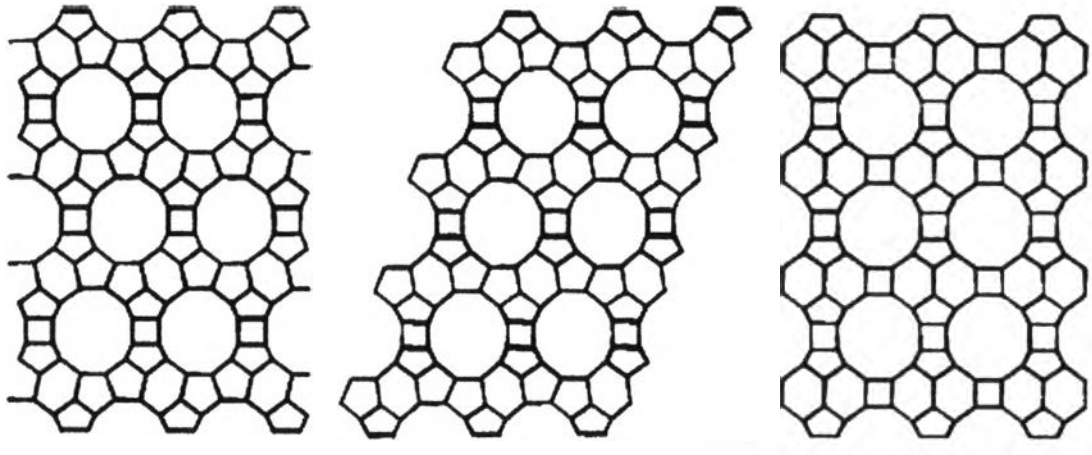

Figure 2.11 Zeolite beta polymorphs [73]

Zeolite beta is an efficient acid catalyst due to the presence of large intersecting pores in a highly siliceous framework. It possesses high thermal and acid treatment stability, high strength acid site and hydrophobic [53]. Examples of successful applications of zeolite beta include aromatic alkylation of biphenyl with propylene [74], indole synthesis, aromatic nitration and aliphatic alkylation. It is effective in lowering the pour point of petroleum oil by isomerizing the normal alkanes to their branched isomers, rather than cracking them to lighter alkanes, as is done by other zeolites such as ZSM-5 and erionite [75]. Zeolite beta was found to be active for cracking of n-hexane [37], polyolefins [11] and pentane hydroisomerization [35]. The shape selective catalytic properties of zeolite beta, especially in the cracking of alkanes and in the isomerization of m-xylene, have recently been investigated [76].

2.3 SBA-15

2.3.1 Structure and Properties of SBA-15

Recently, SBA-15 mesoporous material has been synthesized under acidic condition using triblock copolymer as a structure directing agent. This novel mesoporous material exhibits higher hydrothermal stability as compared to MCM-41 due to its thicker pore walls (3.1-6.4 nm). It also has uniform and hexagonal-structured channel similar to MCM-41 as shown in Figure 2.12 but with larger pore size which makes it more desirable to deal with bulky molecules.

Figure 2.12 Hexagonal mesoporous structure.

MCM-41 and FSM-16 can be synthesized using quaternary ammonium salt as a template. In case of SBA-15, amphiphilic tribock copolymer can be modified as a template and must be synthesized in acid condition of hydrochloric acid. On the other hand, HMS can be prepared in neutral and environmentally benign condition using primary amine as a template. Although these materials have the same hexagonal structure, some properties are different as shown in Table 2.1.

Table 2.1 Properties of some hexagonal mesoporous materials [77-83]

Material	Pore size (Å)	Wall thickness (nm)	BET specific surface area (m^2/g)	Framework structure
MCM-41	15-100	1	>1000	Honey comb
FSM-16	15-32	-	680-1000	Folded sheet
SBA-15	46-300	3-6	630-1000	Rope-like
HMS	29-41	1-2	640-1000	Wormhole

2.3.2 Synthesis and Mechanism for Formation of SBA-15

For SBA-15 materials, aging time and temperature are particularly important. Kruk *et al.* found that mesoporous SBA-15 prepared from calcination of an 'as-prepared' hybrid precursor contained a significant fraction of microporosity; further aging of the precursor in the mother liquors leads to an improvement on the pore size distribution (Figure 2.13), in agreement with the first work by Zhao *et al.* [84].

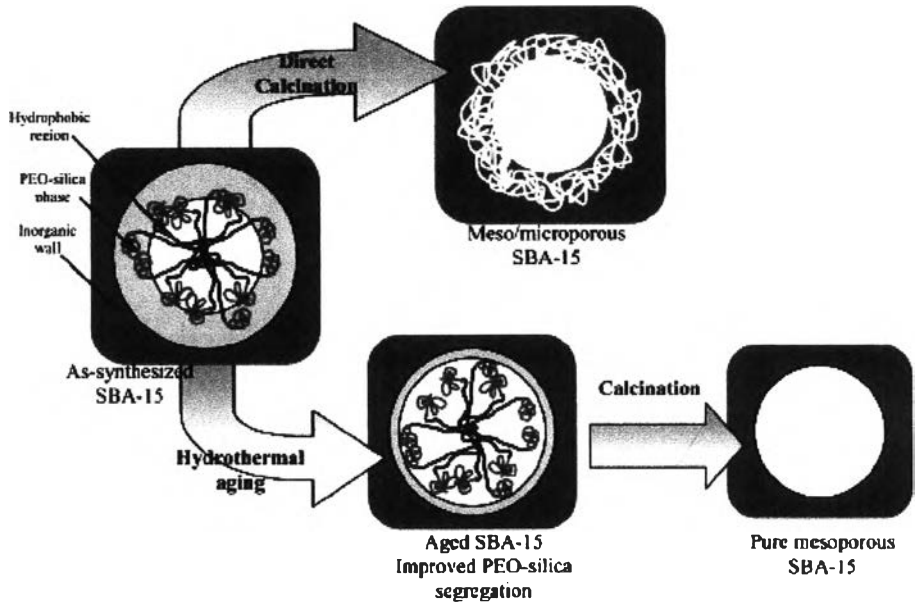

Figure 2.13 Pore evolution upon thermal treatment, depending on pre-treatment and aging [85].

Aging of an as-prepared precipitate at 80–100°C seems to help segregation of the PEO blocks and the inorganic framework, by promoting condensation of the latter. High temperatures also change the polymer behavior. It is known that at temperature above 0°C, PEO blocks become less hydrophilic and expel water (the same is valid for the more hydrophobic PPO blocks, at temperature above 40°C) [85]. For a mechanism, firstly alkoxysilane species (TMOS or TEOS) are hydrolyzed as:

$$Si(OEt)_4 + nH_3O^+ \xrightarrow[pH<2]{\text{hydrolysis}} Si(OEt)_{4-n}(H_2O^+)_n + n\ EtOH$$

which is followed by partial oligomerization at the silicon atom. Furthermore, at this condition, the PEO parts of surfactant associate with hydronium ions as followed:

$$\text{-}PEO_m\text{-} + yHX \xrightarrow{H_2O} \text{-}PEO_{m-y}[(EO).3H_2O^+]_y \text{----}X_y^-$$

Next, coordination sphere expansion around the silicon atom by anion coordination of the form $X^-SiO_2^+$ may play an important role. The hydrophilic PEO blocks are expected to interact with the protonated silica and thus to be closely associated with the inorganic wall. During the hydrolysis and condensation of the silica species, intermediate mesophase is sometimes observed and further condensation of silica species and organization of the surfactant and inorganic species result in the formation of the lowest energy silica-surfactant mesophase structure allowed by solidifying network.

Thus, the block copolymer has been used to solve these problems. Generally, amphiphilic block copolymer has been used in the field of surfactants, detergent manufacturing, emulsifying, coating, etc. The properties of block copolymer can be continuously tuned by adjusting solvent composition, molecular weight, or type of polymers. Figure 2.14 shows typical block copolymer used as templates.

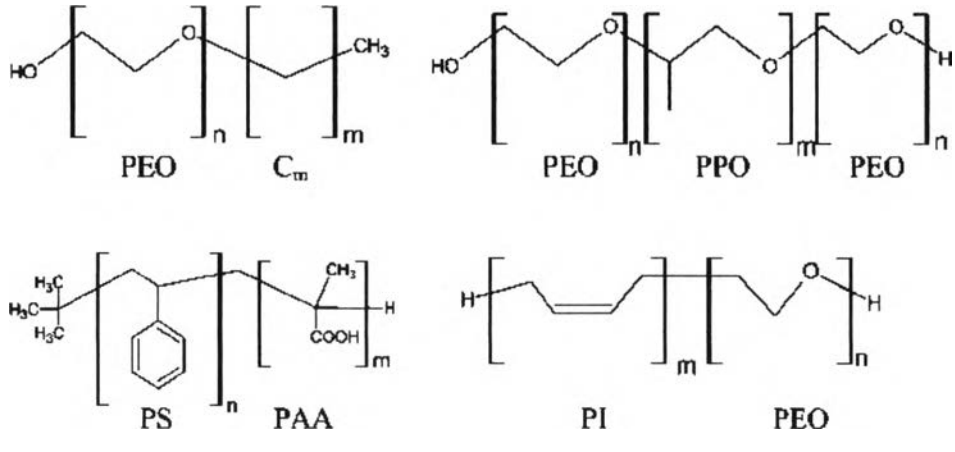

Figure 2.14 Block copolymer used in mesostructured generation [86].

Some advantages of using these block copolymer are:

(1) *The thicker wall thickness* (about 15-40 Å), enhancing hydrothermal and thermal stability of materials.

(2) *Pore diameter can be tuned easier* by varying type or concentration of polymer.

(3) *Easier to remove from mineral framework* by thermal treatment or solvent extraction. Due to the hydrogen bonding interaction between template and

inorganic framework, therefore, it should be easier to dissociate as compared to ionic templates (electrostatic interaction).

Interaction between block copolymer template and inorganic species, called hybrid interphase (HI), is particularly important, especially in PEO-PPO based one. Different possible interactions taking place at the HI are schematized in Figure 2.15. Most of the fine HI characterization has been performed on PEO-based (di or triblock) templates. Melosh *et al.* [86] determined that in F127-templated silica monoliths, organization arose for polymer weight fractions higher than 40%. For lower polymericsilica ratios, non-ordered gels were formed. This lack of order was due to a relatively strong interaction (probably of H-bonding type) of the (Si—O–Si) polymers forming the inorganic skeleton with both PEO and PPO blocks.

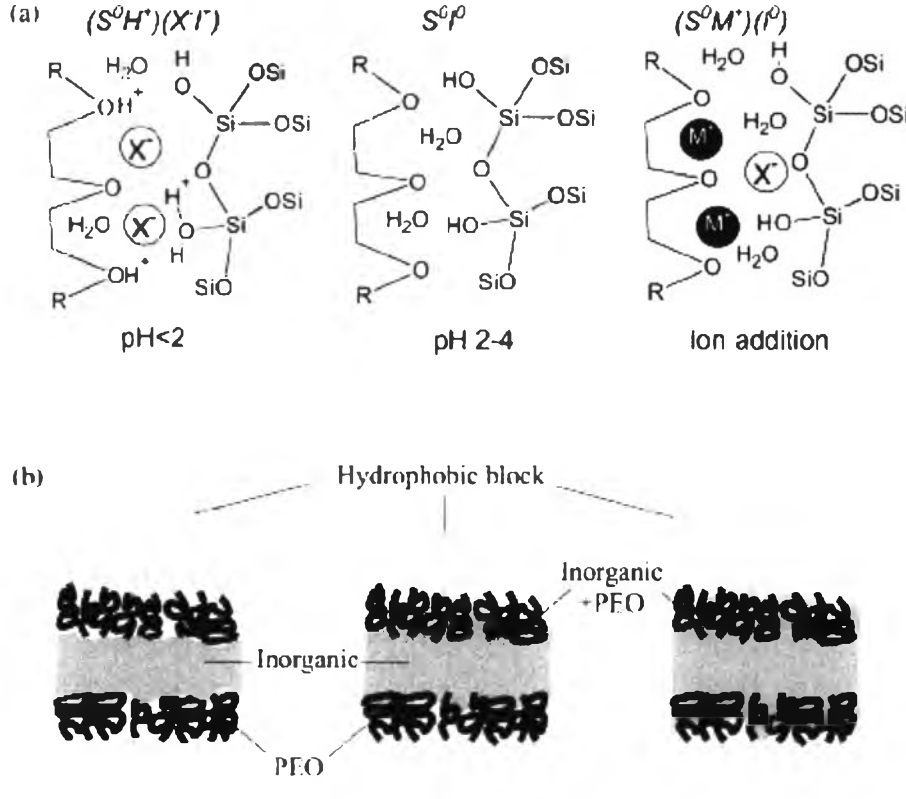

Figure 2.15 (a) Schematic view of the $(S^0H^+)(X^-I^+)$, S^0I^0, and $(S^0M^+)(X^-I^0)$ hybrid interphases (HIs) (b) Three possible structures of a HI composed by a nonionic polymer and an inorganic framework [86].

2.4 Characterization of Mesoporous and Microporous Material

2.4.1 X-ray Diffraction (XRD)

The most frequently used method for identifying and describing structures of zeolite and mesoporous material are the X-ray powder diffraction (XRD). The simplicity of the powder diffraction technique is easily applied to the small structure of zeolites where single crystal method cannot be used. X-rays are electromagnetic radiation of very short wavelength about 1 Å that occurs between gamma-rays and ultra-violet on the electromagnetic spectrum. This wavelength is approximately the same length as the diameter of an atom, making it ideally suitable for probing the structural arrangement of atoms and molecules in a wide range of materials. The energetic X-rays penetrate deep into the materials and provide information about the bulk structure. X-rays are produced generally by either X-ray tubes radiation. In a X-ray tube, which is the primary X-ray source used in laboratory instruments, X-rays are generated when a focused electron beam, accelerated across a high voltage field bombards a stationary or rotating solid target. As electrons collide with atoms in the target and slow down, a continuous spectrum of X-rays are emitted. The high energy electrons also eject inner shell electrons from the atoms through the ionization process. When a free electron fills the shell, an X-ray photon, with energy characteristics equal to the target material, is emitted. Common targets used in X-ray tubes include Cu and Mo, which emit wavelengths of 1.54 Å and 0.8 Å, respectively. The energy E of an X-ray photon and it's wavelength (λ) are relate by Equation 2.1

$$E = \frac{hc}{\lambda} \qquad 2.1$$

Where h is Planck's constant and c is the speed of light.

Diffracted waves from different atoms can interfere with each other. The resultant intensity distribution is strongly affected by this interaction. If the atoms are arranged in a periodic fashion, as in crystals, the diffracted waves will consist of sharp interference peaks with the same symmetry as in the distribution of atoms. Thus, the distribution of atoms in material can be deduced by measuring the diffraction pattern. Powder X-ray Diffraction (XRD) is perhaps the most widely used XRD technique for characterizing materials. This technique is also used widely for studying particles in liquid suspensions or polycrystalline solid (bulk or thin film material). The term

powder simply means that the crystalline domains are randomly oriented in the sample. When the 2-D diffraction pattern of recorded, it displays concentric rings of scattering peaks corresponding to the various spacing (d) in the crystal lattice. The positions and the intensities of the peaks are used for identifying the underlying structure (or phase) of the material. For example, the diffraction line of graphite would be different from diamond even though they both are made of carbon atoms. This phase identification is important because the material properties are highly dependent on structure. The peaks in X-ray diffraction pattern are directly related to atomic distances. Therefore, the size and shape of the unit cell for any compound can easily be determined using the path difference between two waves. Equation 2.2 gives the path difference between two wavelengths. It is geometrically derived using the laws of diffraction as shown in Figure 2.16.

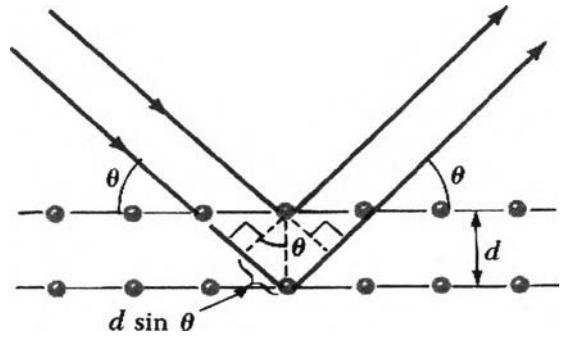

Figure 2.16 Geometric derivation of Bragg's law

$$\lambda = 2d\sin\theta \qquad 2.2$$

However, for constructive interference between these waves, the path difference must be an integral number of wavelengths, which leads to:

$$2d\sin\theta = n\lambda \qquad 2.3$$

Equation 2.3 is known as the Bragg's law, where λ is the wavelength of X-ray, θ the scattering angle, and n an integer representing the order of the diffraction peak. Bragg's law is one of most important laws used for interpreting X-ray diffraction data.

Bragg's law applied to scattering centers consisting of any periodic distribution of electron density. In other words, the law holds true if the atoms are replaced by molecules or collections of molecules, such as colloids, polymers, proteins and virus particles. From XRD spectra an important correlation of the peak broadening with the crystal size can be calculated using the Scherrer equation:

$$D = \frac{k\lambda}{\beta \cos\theta}$$

Where D is the crystal size in angstroms, k is a constant approximately equal to unity if β is the half-maximum peak breadth in radians, λ is the wavelength of the X-rays in angstroms, and θ is the Bragg angle of the same peak used to calculate β [87].

Using this method, Braggs' law is able to determine the interplanar spacing of the samples, from diffraction peak according to Bragg angle.

$$n\lambda = 2\, d \sin\theta$$

Where the integer *n* is the order of the diffracted beam, λ is the wavelength; *d* is the distance between adjacent planes of atoms (the *d*-spacings) and θ is the angle of between the incident beam and these planes.

2.4.2 Scanning Electron Microscopy (SEM)

The scanning electron microscope (SEM) provides valuable information about the microstructure characteristics of material including the morphology, purity and homogeneity of the final product. Small amounts of amorphous material that cannot be detectable by XRD are more easily distinguished. SEM investigation leads to important information of crystal shape, size and distribution, the nature of inner-growth and over-growth crystalline impurities [88]. The SEM creates magnified images by using electrons instead of light waves as used by traditional microscopes. The SEM shows very detailed 3-dimentional black and white images at much higher magnification than is possible with a light microscope. If the samples are not made out of a conductive material, the samples are coated with a very thin layer of gold by a

machine called a sputter coater. The sample is placed inside the microscope's vacuum column trough an airtight door. After the air is pumped out of the column, an electron gun emits a beam of high-energy electrons from the top. This beam travels downward through a series of magnetic lenses designed to focus the electrons to a very fine spot. Near the bottom, a set of scanning coil moves the focused beam back and forth across the specimen, row by row. As the electron beam hits each spot on the sample, secondary electrons are knocked loose from its surface. A detector counts these electrons and sends the signals to an amplifier. The final image is built up from the number of electrons emitted from each spot on the sample. The morphology of SBA-15 and zeolite beta can be easily observed in SEM as Figure 2.17.

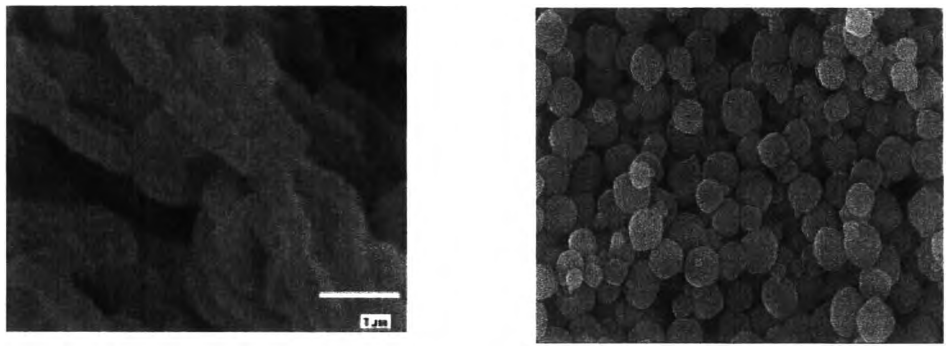

Figure 2.17 Scanning electron micrograph of (a) SBA-15 (b) zeolite beta sample.

2.4.3 Nitrogen Adsorption-Desorption Isotherm

The N_2 adsorption technique is used to determine the physical properties of mesoporous microporous molecular sieves, such as the surface area, pore volume, pore diameter and pore-size distribution of solid catalysts. Adsorption of gas by a porous material is described by an adsorption isotherm, the amount of adsorbed gas by the material at a fixed temperature as a function of pressure. Porous materials are frequently characterized in terms of pore sizes derived from gas sorption data. IUPAC conventions have been proposed for classifying pore sizes and gas sorption isotherms that reflect the relationship between porosity and sorption. The IUPAC classification of adsorption isotherms is illustrated in Figure 2.18. Six types of isotherms are characteristic of adsorbents that are microporous material like zeolite (type I). Typical type I isotherm always show high capacity and very fast reaction saturation, followd

by consistent adsorption over a wide range of P/P_0. Nonporous materials exhibit the adsorption isotherm type II while type III isotherm is for macroporous materials. Adsorption isotherm for nonporous materials show high adsorption capacity at low relative pressure (P/P_0), moderate adsorption capacity at middle and high adsorption capacity at P/P_0 in proximity to 1. Type IV isotherm show a characteristic of mesoporous materials. Type V isotherm represent when the interaction of molecule of nitrogen are stronger than the interaction of nitrogen with solids. Type VI represents nonporous material which has uniform surface.

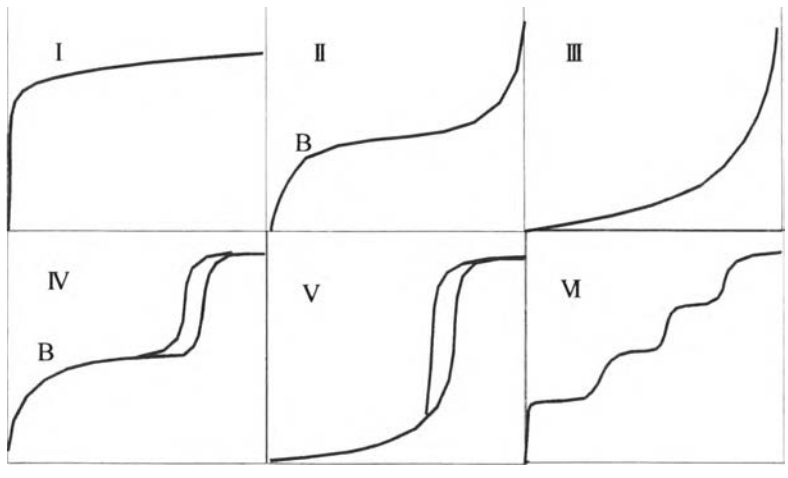

Figure 2.18 The IUPAC classification of adsorption isotherm. [89]

Adsorption isotherms are described as shown in Table 2.2 based on the strength of the interaction between the sample surface and adsorptive. Pore types are classified as shown in Table 2.3. Pore size distribution is measured by the use of nitrogen adsorption/desorption isotherm at liquid nitrogen temperature and relative pressure (P/P_o) ranging from 0.05-0.1.The large uptake of nitrogen at low P/P_o indicates filling of the micropore (<20Å) in adsorbent. The linear portion of the curve represents multilayer adsorption of nitrogen on the surface of the sample, and the concave upward portion of the curve represents filling of mesoporous and macropores.

Table 2.2 Features of adsorption isotherms [90]

Type	**Interaction between sample surface and gas adsorbate**	**Porosity**	**Example of adsorbate**
I	Relatively strong	Micropores	Activated carbon-N_2
II	Relatively strong	Nonporous	Oxide-N_2
III	Weak	Nonporous	Carbon-water vapor
IV	Relatively strong	Mesopore	Silica-N_2
V	Weak	Micropores Mesopore	Activated carbon-water vapor
VI	Relatively strong Sample surface has an even distribution of energy	Nonporous	Graphite-Kr

Table 2.3 IUPAC classification of pores [91]

Pore Type	Pore diameter / nm
Micropore	Up to 2
Mesopore	2 to 50
Macropore	50 to up

Pore size distribution is measured by the use of nitrogen adsorption/desorption isotherm at liquid nitrogen temperature and relative pressures (P/P_o) ranging from 0.05-0.1. The large uptake of nitrogen at low P/P_o indicates filling of the micropores (<20 Å) in the adsorbent. The linear portion of the curve represents multilayer adsorption of nitrogen on the surface of the sample, and the concave upward portion of the curve represents filling of mesopores and macropores. Specific surface area and the porosity of catalysts can be determined by applying the nitrogen adsorption and desorption method at the temperature of liquid nitrogen. The surface area of powder or solid can be calculated using the multipoint Brunauer, Emmett and Teller (BET) [92] method is commonly used to measure total surface area.

$$\frac{1}{w\left(\frac{P_o}{P}-1\right)} = \frac{1}{W_m C} + \frac{C-1}{W_m C}\left(\frac{P}{P_o}\right)$$

Where W is the weight of nitrogen adsorbed at the equilibrium pressure P; P_o is the vapour pressure at saturation of the adsorbate at the adsorption temperature; and W_m is the weight of adsorbate constituting a monolayer of surface coverage. The BET constant C is related to the heat of adsorption corresponding to the first layer of adsorbate and to the heat of condensation of adsorbate. Therefore, its value is an indication of the magnitude of the adsorpbent/adsorbate interactions. A multi-point linear plot was developed by using

$$\frac{1}{\left[W\left(\frac{P_o}{P}-1\right)\right]} \quad vs \quad \frac{P}{P_o} \qquad 1$$

For most solids this plot is restricted to a limited region of adsorption isotherm where the slope is linear: in this study the P/P_o range was limited to between 0.05 to 0.30. The value of W_m is obtained from the slope $P/W(P^o-P) = f(P/P^o)$, which is equal to $C-1/W_m$, and from the coordinates of the origin $1/W_mC$.

The weight of a monolayer of adsorbate (W_m) is obtained from the slope (m) and the intercept (I) of the BET plot:

$$m = \frac{C-1}{W_m C} \qquad 2$$

$$I = \frac{1}{W_m C} \qquad 3$$

Thus, the weight of the monolayer (W_m) is obtained by combining equations 2 and 3:

$$W_m = \frac{1}{m+I} \qquad 4$$

Finally, the surface area is calculated by using the molecular cross-sectional area (A_{cs}) of the adsorbate molecule. The total surface area (S_t) of a solid sample is expressed as:

$$S_t = \frac{W_m N A_{cs}}{M} \qquad 5$$

Where N is Avogadro's number (6.023 x 10^{23} molecule/mole) and M is the molecular weight of the adsorbate. The most common gas adsorbate used for BET surface are determination is nitrogen. For the hexagonal close-packed nitrogen monolayer at 77 K, the cross-sectional area (A_{cs}) for nitrogen is 16.2 A^2 [92].
The specific surface area (S) of the solid is calculated from the total surface area (S_t) and the sample weight (w) according to Equation 6:

$$S = \frac{S_t}{w} \qquad 6$$

2.4.4 Temperature-Programmed Desorption (TPD) of Ammonia

Temperature-Programmed Desorption (TPD) is one of the most widely used and flexible techniques for characterizing the tolal surface acidity and acid strength of the acidic zeolite catalysts. The following assumptions are made regarding the adsorption and desorption of ammonia molecule:

(i) The intracrystalline zeolite surface is homogeneous and amount of ammonia adsorbed in the experiment is less than that required for a monolayer coverage,

(ii) No readsorption of ammonia takes place during the desorption stage and

(iii) There is no lateral interaction between the neighboring adsorbed ammonia molecules.

The temperature of furnace was monitored by a multi-program controller. The desorption of ammonia was carried out gradually by heating the catalyst from 80°C to 600°C in a flow of helium at 20 ml/min and according to a linear heating program at a rate of 10°C/min. The desorbed ammonia was measured by a thermal conductivity detector.

The NH_3-TPD thermogram profile obtained qualitatively showed the amount of ammonia desorbed at increasing temperature intervals which corresponds to the distribution of acid strengths of the total surface acidity. Figure 2.19 shows the NH_3-TPD thermogram of zeolite beta. The thermograms of the samples present two peaks at low and high temperatures. The intensity of the high temperature desorption peak is related to the desorption of ammonia from strong acid sites whereas the low temperature peak characterized the desorption of the base from weak acid sites. At low region of acid sites consists of physically bonded ammonia to the surface of catalysts or known as physisorbed ammonia and at higher region, the acid sites consist of chemically bonded ammonis with the catalysts which is called chemisorbed [93].

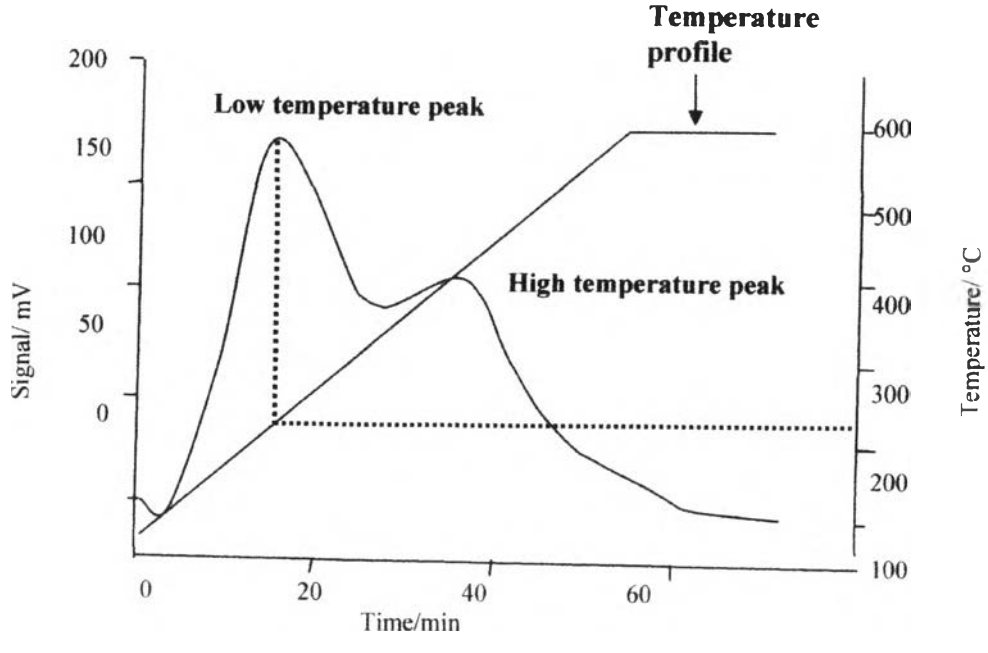

Figure 2.19 NH_3-TPD profiles of zeolite beta sample

2.4.5 ^{27}Al-MAS-NMR

Another important characterization technique for mesoporous materials is solid state NMR. ^{27}Al-MAS-NMR spectroscopy has been employed to distinguish between tetrahedrally and octahedrally coordinated aluminum in the framework at approximately 50 and 0 ppm, respectively. Hence, the amount of framework aluminum can be determined [94].

2.5 Cracking Process

Cracking is the name given to breaking up large hydrocarbon molecules (lower value stock) into smaller and more useful bits (light and middle distillate). This is achieved by using high pressures and temperatures without a catalyst (thermal cracking or pyrolysis), or lower temperatures and pressures in the presence of a catalyst (catalytic cracking). In refinery, the source of the large hydrocarbon molecules is often the naphtha fraction or the gas oil fraction from the fractional distillation of crude oil (petroleum). These fractions are obtained from the distillation process as liquids, but are re-vaporized before cracking. There is not any single unique reaction happening in the cracker. Any acid would do, but in a conventional chemical reaction of hydrocarbons with a strong acid (e.g., H_2SO_4), it would be kind of difficult both to separate out what we wanted afterward and avoid corroding cracking reactors. Thus, the catalysts used are solids with acidic surfaces, so they stay where they are put. A major difference between thermal cracking and catalytic cracking is that reaction through catalytic cracking occurred via carbocation intermediate, compared to the free radical intermediate in thermal cracking as shown in Figure 2.20. Carbocation has longer life and accordingly more selective than free radicals, therefore, the catalytic cracking product can be controlled more easily than those of thermal cracking.

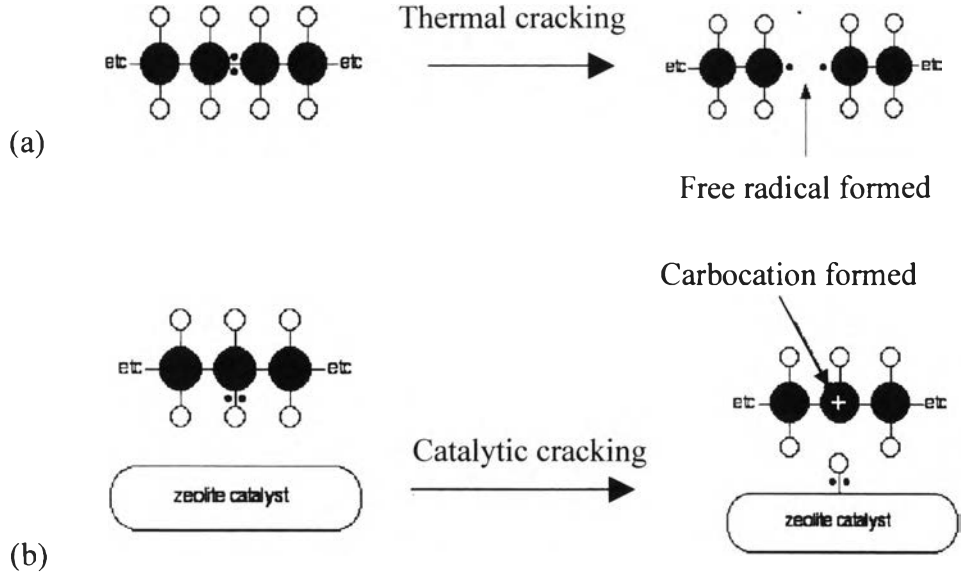

Figure 2.20 Model for cracking of hydrocarbon via (a) thermal cracking and (b) catalytic cracking.

2.5.1 Thermal Cracking of Polyolefins

The non-catalytic or thermal pyrolysis of polyolefins is a high energy, endothermic process requiring temperatures of at least 350-500°C [95-96]. In some studies, temperatures as high as 700-900°C are essential in achieving decent product yields [97-98]. Thermal pyrolysis of both virgin and waste plastics as well as other hydro-carbonaceous sources has been studied extensively in the past. A good number of these thermal cracking studies are on PE [98], polystyrene (PS) [99], and PP [100]. On the other hand, only a few have researched the thermal decomposition of other common plastics such as polyvinylchloride (PVC) ([101]), polymethyl methacrylate [102], polyurethane [103], and polyethylene terephthalate [104].

2.5.1.1 The Hydrocarbon Cracking Mechanism

A thorough study on the mechanism for the thermal decomposition of polymers is presented by Cullis and Hirschler [105]. The four mechanisms proposed are:

(1) End-chain scission or unzipping: Cracking is targeted at chain ends first, and then successively works down the polymeric length. Unzipping results in the production of the monomer.

(2) Random-chain scission: Random fragmentization of polymer along polymer length. Results in both monomers and oligomers.

(3) Chain-stripping: Side chain reactions involving substituents on the polymer chain.

(4) Cross-linking: Two adjacent 'stripped' polymer chains can form a bond resulting in a higher MW species. An example is char formation.

The thermal pyrolysis of PP and PE is known to follow the random chain scission route, resulting in mainly oligomers and dimers [106]. This mechanism is illustrated for PE and PP in Figures 2.21 and 2.22, respectively. Peterson *et. al.* observed that PE decomposition by thermogravimetry yielded mainly 1-hexene and propene [107].

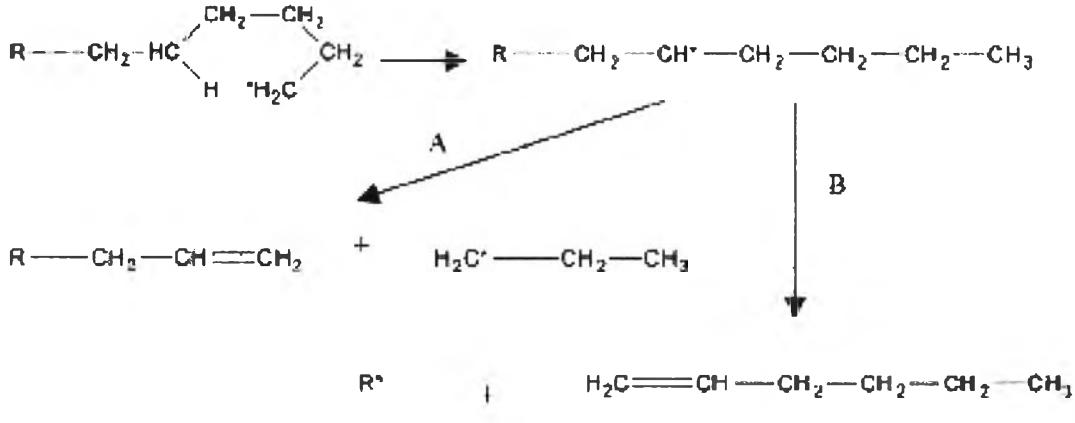

Figure 2.21 Random chain scission in polyethylene

Similarly Peterson *et. al.* observed that in the thermal pyrolysis of PP, the main products were pentane, 2-methyl-1-pentene and 2,4 dimethyl 1-heptene [107]. During degradation, methyl, primary and secondary alkyl radicals are formed, and by hydrogen abstractions and recombination of radical units, methane, olefins and monomers are produced [108].

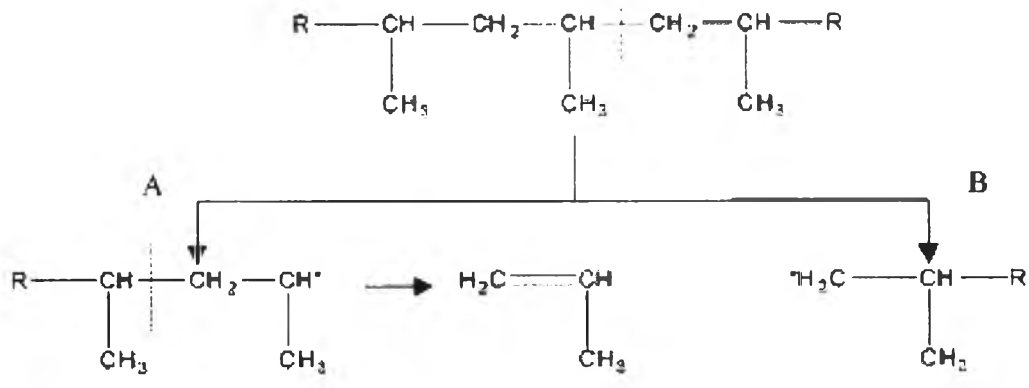

Figure 2.22 Random chain scission in polypropylene [107]

Polyolefin samples are typically degraded in a closed reactor/melting vessel and heated to a reaction temperature at which the polymer decomposes. A reaction time is allowed and over time, the degradation products (gaseous, liquids and solid) are collected and an Common methods for liquid products analyses include Infra–Red (IR), Mass Spectros (MS) and gas chromatography (GC). Whereas gaseous products are analyzed typically by Nuclear Magnetic Resonance (NMR), Fourier Transform Infrared Spectroscopy (FTIR) and GC/MS. Solid residues are identified by gel permeation chromatography. Several couplingof the aforementioned analytical methods are available, including FTIR/MS and GC/MS

A large number of chemical reactions take place during steam cracking, most of them based on free radicals. Computer simulations aimed at modeling what takes place during steam cracking have included hundreds or even thousands of reactions in their models. The main reactions that take place include:

1. Initiation reactions, where a single molecule breaks apart into two free radicals. Only a small fraction of the feed molecules actually undergo initiation, but these reactions are necessary to produce the free radicals that drive the rest of the reactions. In steam cracking, initiation usually involves breaking a chemical bond between two carbon atoms, rather than the bond between a carbon and a hydrogen atom.

$$CH_3CH_3 \rightarrow 2\ CH_3\bullet$$

2. Hydrogen abstraction, where a free radical removes a hydrogen atom from another molecule, turning the second molecule into a free radical.

$$CH_3\bullet + CH_3CH_3 \rightarrow CH_4 + CH_3CH_2\bullet$$

3. Radical decomposition, where a free radical breaks apart into two molecules, one an alkene, the other a free radical. This is the process that results in the alkene products of steam cracking.

$$CH_3CH_2\bullet \rightarrow CH_2{=}CH_2 + H\bullet$$

4. Radical addition, the reverse of radical decomposition, in which a radical reacts with an alkene to form a single, larger free radical. These processes are involved in forming the aromatic products that result when heavier feedstocks are used.

$$CH_3CH_2\bullet + CH_2{=}CH_2 \rightarrow CH_3CH_2CH_2CH_2\bullet$$

5. Termination reactions, which happen when two free radicals react with each other to produce products that are not free radicals. Two common forms of termination are *recombination*, where the two radicals combine to form one larger molecule, and *disproportionation*, where one radical transfers a hydrogen atom to the other, giving an alkene and an alkane [109].

$$CH_3\bullet + CH_3CH_2\bullet \rightarrow CH_3CH_2CH_3$$
$$CH_3CH_2\bullet + CH_3CH_2\bullet \rightarrow CH_2{=}CH_2 + CH_3CH_3$$

2.5.1.2 Thermal Pyrolysis Product Yields

product yields greater than 82.5% and as high as 96% have been observed for PE pyrolysis [110]; however, these were obtained at high temperatures (greater than 420°C) and within a reaction time of approximately one hr. Invariably, the gaseous products obtained by thermal cracking are not suitable for use as fuel products, requiring further refining to be upgraded to useable fuel products [111].Generally, thermal cracking results in liquids with low octane value and higher residue contents at moderate temperatures, thus making the process an inefficient process for producing gasoline range fuels. A few researchers have sought to improve thermal pyrolysis of waste polyolefins without employing the use of catalysts; however, these changes either yielded insignificant improvements or added another level of complexity and costs to the system [112].

2.5.2 Catalytic Cracking of Polyolefins

Catalytic degradation of polymers has shown the greatest potential to be developed into a comercialized process. In comparison to the purely thermal pyrolysis, the addition of catalysts in polyolefin pyrolysis:

- Significantly lowers pyrolysis temperatures. A significant reduction in degradation temperature and reaction time under catalytic conditions results in an increase in the conversion rates for a wide range of polymers at much lower temperatures than with thermal pyrolysis [113].
- Narrows and provides better control over the hydrocarbon (HC) products distribution in LDPE [114] , HDPE , PP[115] and PS [116] pyrolysis. While thermal pyrolysis results in a broad range of HCs ranging from C_5 to C_{28} [96], the selectivity of products in the gasoline range (C_5-C_{12}) are much more enhanced by the presence of catalysts [11, 113].
- Increases the gaseous product yields. Under similar temperatures and reaction times, a much higher gaseous product yield is observed in the presence of a catalyst for PE [113, 117].
- Increases the product yield in the gasoline range whereas a purely thermal process will produce more light gas oils [118]. Zeolites in particular are

known to enhance the formation of branched hydrocarbons and aromatics [119]. Oils obtained by catalytic pyrolysis contain less olefins and more aromatic content [120].

2.5.2.1 Catalytic Cracking Mechanisms

In general, for components with equal carbon numbers, the rate of cracking decreases in the order: i-olefins > n-olefins > i-paraffins ≈ naphthenes > n-paraffins > aromatics. The cracking mechanism can be seen as a chain mechanism that involves the intermediate formation of carbocations, positively charged hydrocarbon species. Carbocations include both carbenium ions (e.g. $R_1–CH_2–C^+H–R_2$, $R_1–CH=C^+–R_2$) and carbonium ions (e.g. $R_1–CH_2–C^+H_3–R_2$, $R_1–CH=C^+H_2–R_2$). In carbenium ions, the charge carrying carbon atom can be di- or tri-coordinated, while in carbonium ions, the charge carrying carbon atom is tetra- or pentacoordinated. The stability of the carbocations decreases in the order tertiary > secondary > primary [121]. Cracking of hydrocarbons is primary a reaction that proceeds through adsorbed carbenium ion intermediates.

2.5.3. Reactions of Olefins

The formation of carbenium ions from olefins can easily proceed by addition of the proton from a Brønsted acid site of the catalyst to the carbon–carbon double bond. Cracking of the adsorbed carbenium ion proceeds through the β-scission mechanism [122-123] or through the protonated cyclopropane mechanism [124]. An illustration is given in Fig. 2.23.

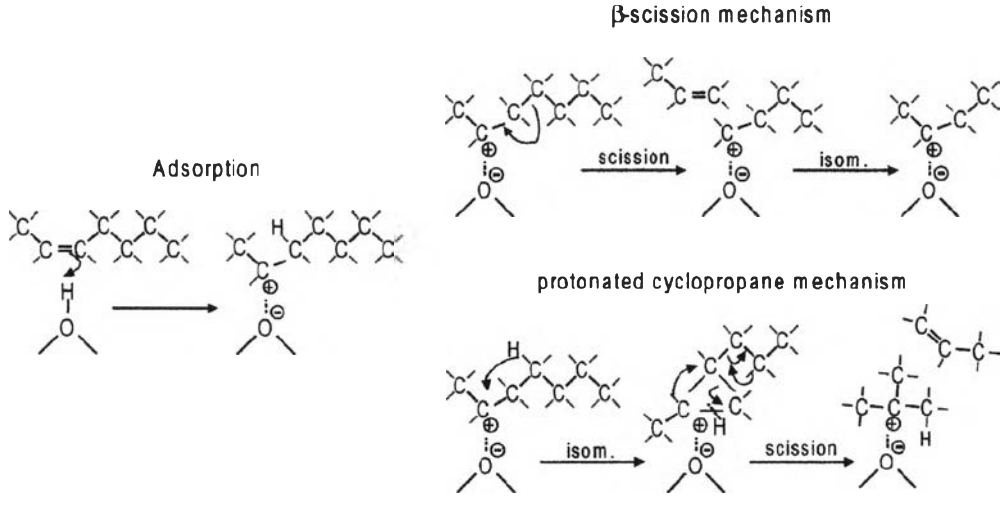

Figure 2.23 Cracking mechanisms illustrated by the reaction of n-heptene; adsorption at a Brønsted acid site leads to formation of an adsorbed carbenium ion that can be cracked. Both the β-scission mechanism [122-123] and the protonated cyclopropane mechanism [124] are shown.

Other reactions of the adsorbed carbenium ion are [125-126]:

1. Isomerization to a more stable carbenium ion, for example, through a methyl shift:

$$R_1\text{–}CH_2\text{–}C^+H\text{–}R_2 \rightarrow R_1\text{–}\underset{\displaystyle CH_3}{\overset{\displaystyle |}{C^+}}\text{–}R_2 + H^+ \qquad (1)$$

2. Oligomerization with olefin in a bimolecular reaction to form a larger adsorbed carbenium ion:

$$R_1\text{–}C^+H\text{–}R_2 + R_3\text{–}CH{=}R_4 \rightarrow R_1\text{–}\underset{\displaystyle R_3\text{–}CH_2\text{–}CH\text{–}R_4}{\overset{\displaystyle |}{C^+}}\text{–}R_2 \qquad (2)$$

3. Desorption with deprotonation to form an olefin (the opposite of adsorption):

$$R_1\text{–}CH_2\text{–}C^+H\text{–}R_2 \rightarrow R_1\text{–}CH{=}CH\text{–}R_2 + H^+ \qquad (3)$$

4. Desorption with hydride abstraction from a paraffin to form new paraffin from the carbenium ion and new carbenium ion from the paraffin (H-transfer reaction):

$$R_1–C^+H–R_2 + R_3–CH_2–R_4 \rightarrow R_1–CH_2–R_2 + R_3–C^+H–R_4 \quad (4)$$

5. Desorption with hydride abstraction from (cyclic) olefins or coke (precursors) to form paraffin and a more aromatic compound (H-transfer reaction):

$$R_1–C^+H–R_2 + R_3–HC=CH–R_4 \rightarrow R_1–CH_2–R_2 + R_3–C^+=CH–R_4 \quad (5)$$

The bimolecular reactions (2), (4) and (5) can occur if the pore size of the catalyst is large enough to accommodate the reactive intermediates, or they should occur on the outer surface of the zeolite particles. If the pores are too small, as in the case of ZSM-5 (0.53 nm× 0.56 nm), these reactions cannot take place with the larger (gasoline) components, although oligomerization or dimerization of small (C_2–C_4) olefins could be possible. For example, in the Mobil olefins to gasoline and distillates process (MOGD) coupling of light hydrocarbons is catalyzed by ZSM-5.

With ZSM-5, cracking through dimeric intermediates has only been reported in the reactions of relatively small *n*-olefins (C_4–C_6). Abbot and Wojciechowski [127] have studied cracking of *n*-olefins from C_5 to C_9 at 678K with ZSM-5 and found that cracking of pentene solely took place through a dimeric/disproportionation mechanism. Cracking of heptene and larger molecules proceeded mainly through monomolecular cracking and at 678 K; hexene represented the transition case of the two mechanisms and was cracked by both monomolecular cracking and through dimeric intermediates.

With Y-type zeolites, the dimeric mechanism is a more important reaction route; for example, it has been found that cracking of C_7 took place for 25% via a dimeric disproportionation reaction at 746K and for 32% at 673K.

2.5.4. Proposed Cracking Mechanisms of Polymer

For ZSM-5 the cracking reactions of larger C_7^+ olefins are restricted to simple β-scission reactions. The relatively straight chains (or parts of it) can enter the pores of ZSM-5, are adsorbed, split-off small olefins, and desorb. For example, the reaction of n-heptene over ZSM-5 (for simplicity only the β-scission mechanism) is shown in Fig.2.24. The adsorbed C_7-carbenium ion is cracked to propene and C_4-carbenium ion. Then C_4-carbenium isomerizes to butene or is cracked to two ethene molecules [128].

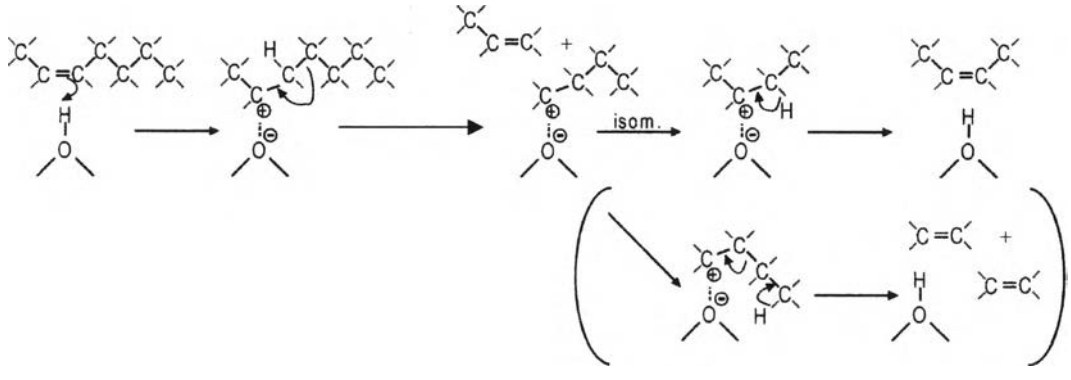

Figure 2.24 Monomolecular cracking mechanisms (only mechanism possible with ZSM-5).

Generally, the second reaction, formation of ethene, is energetically less favorable because it involves the formation of two primary carbenium ions. However, due to the small pores of ZSM-5, the electrical field in the pores is larger and a relatively large interaction between the catalyst and the adsorbed carbenium ions shall exist. It is believed that the oxygen atoms of a zeolite structure play a role in solvating carbocations, delocalizing the positive charge into the framework. The smaller the size of the pores of the zeolite, the closer the different oxygen atoms are to the adsorbed reaction intermediates and the higher the possible interaction. So possibly, as a result of increased stabilization of the intermediates, the formation of ethene is enhanced when small pore-zeolites such as ZSM-5 are involved.

On the base catalyst, with zeolite Y as active species (pore size 0.74 nm) adsorbed C_4-carbenium species and new heptene molecule to form an adsorbed C_{11}-carbenium ion. The C_{11} carbenium ion is cracked to hexane and C_5-carbenium ion.

This bimolecular cracking mechanism proposed by Williams *et al.* [125] is illustrated in Fig. 2.25. Also, the adsorbed heptene carbenium ion could oligomerize before cracking.

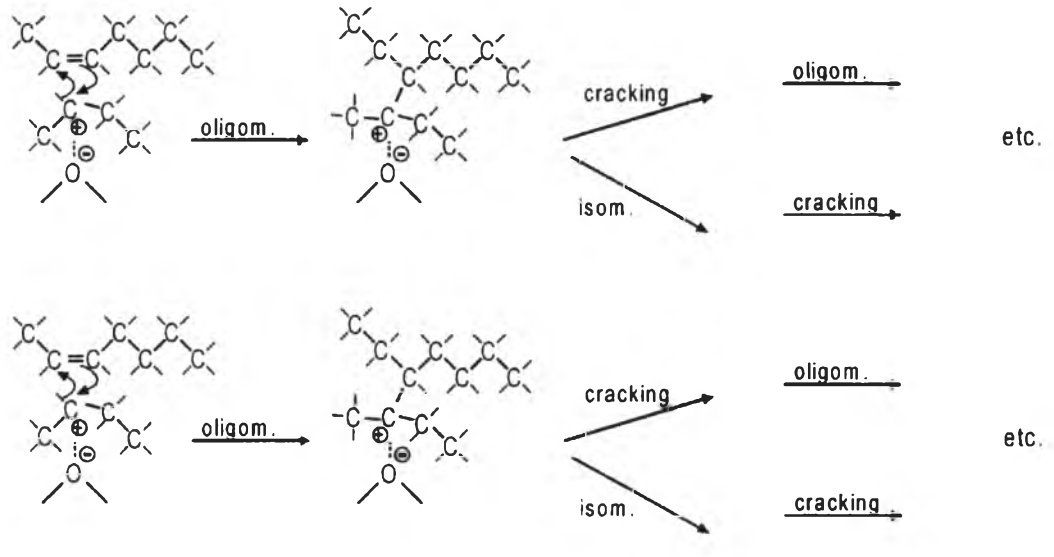

Figure 2.25 Bimolecular cracking mechanism that can occur on zeolite Y in addition to the monomolecular mechanism.

Because of the larger adsorption strength of larger hydrocarbons, the bimolecular mechanism have an important contribution in the cracking mechanism of the heavier gasoline-range olefins, provided that the catalyst pore size is large enough to accommodate the reaction intermediates. Aromatics and highly branched components, therefore, are too large to react through bimolecular mechanisms. Linear components are the most likely ones to react through this mechanism.

According to this proposed mechanism, the active site of ZSM-5 is the acid site itself, while the active site in zeoltie Y can be represented by the adsorbed carbenium ion. The reaction intermediates with ZSM-5 contain the number of carbon atoms (C_5–C_{11}), while the (surface) intermediates with the base catalyst can be much larger. As a result, the cracking products from ZSM-5 will be mainly C_3, C_4, and to some extent also C_2 olefins, while with the zeolite Y base catalyst larger fragments can be formed.

This agrees with the results that can be found in literature; the main products from *n*-olefins and *i*-olefins cracking on ZSM-5 are light olefins with a high

selectivity for propene, *i*-butene, and in some cases the increased yields of ethene are reported.

A mechanism for the catalytic cracking of PE and PP using Al-MCM-41 as catalyst is proposed by Ishihara *et al.* [129-130]. As described, branched polyethylene components have short chains consisted of mainly of methyl groups.

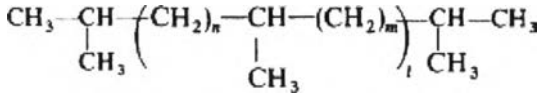

Where n+m=5, m=0-5
and l=2.3-6.7

Branching of the main fraction was at a frequency of one branch per three ethylene monomer units. The typical oligomer structure was found to be virtually the same as that of polyisoheptyl based on branching frequency. Moreover, oligomer chains showed random branching in an ethylene sequence in regular structures of polyisoheptyl. The catalytic cracking of PE is initiated by attack of low molecular weight carbonium ion (R^+) on a very small number of on-chain hydrogen atoms attached to tertiary carbon atoms in polymer chains. The initial reaction of molecular weight reduction is shown in equations (1). β-scission of on-chain carbonium ions (A) occurs to produce chain-ends (B) and (C):

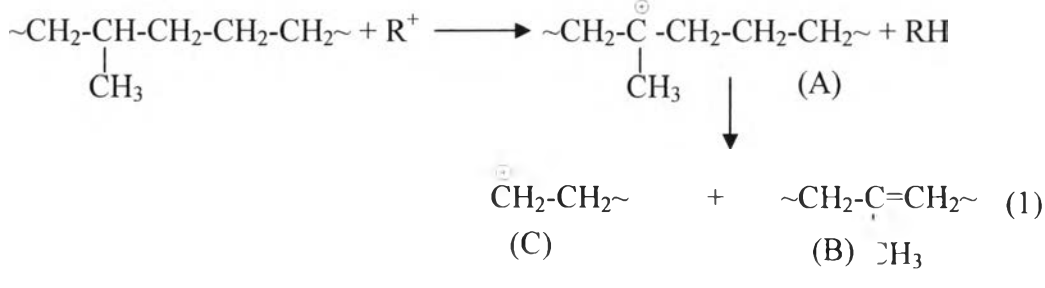

(1)

2.5.4.1 Mechanism of Gas Formation.

Gaseous products are produced from the liquid fraction produced by decomposition of oilgomers and reaction with typical oilgomers is shown in the following scheme. (where R^+ represents the volatile carbonium ion, $\sim CH_2\text{-}\overset{\oplus}{C}H\text{-}CH_2$)

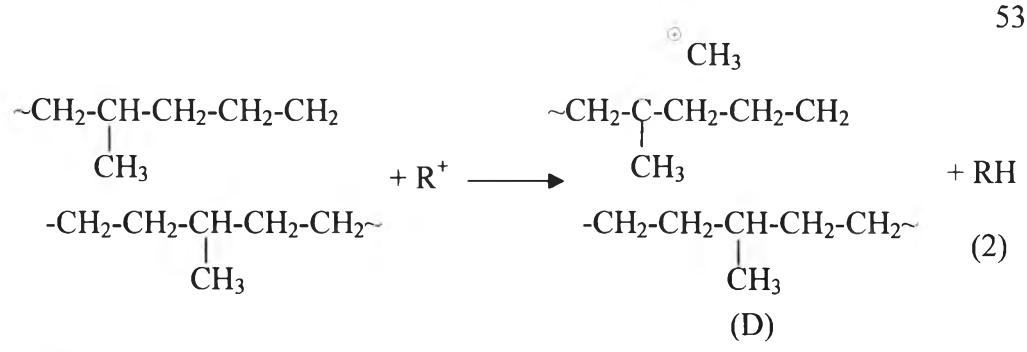

(2)

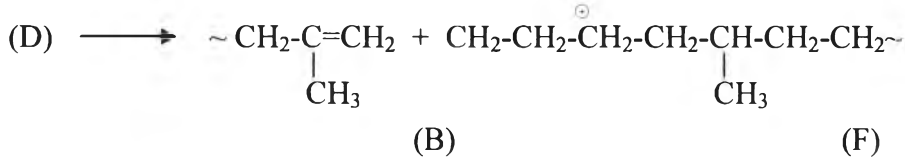

(3)

Gas formation takes place by way of the decomposition of these fractions. The unstable reaction intermediate (F) isomerized to secondary (G) or tertiary carbonium ions (H) as shown by equation (4).

From (F)

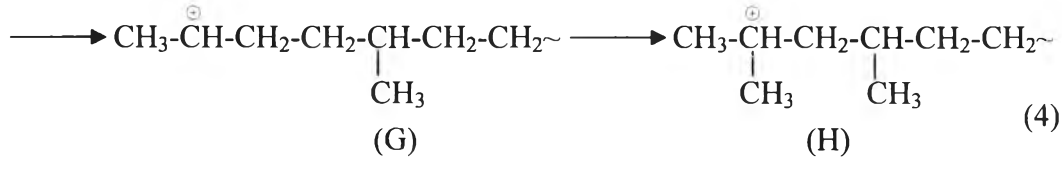

(4)

From (G)

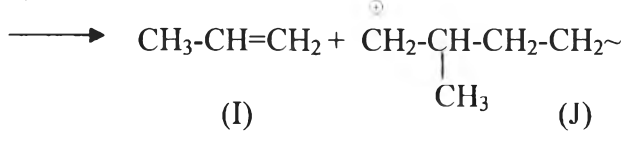

(5)

From (H)

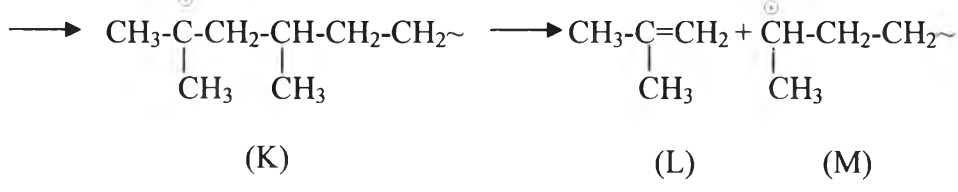

(6)

Ions (G) and (H) are essential to gaseous product formation and are mainly produced by β-scission of these carbonium ions (H). Isobutene is converted to isobutane through hydrogen transfer by the catalyst so that its yield is remarkably high. Propylene is produced in high yield by direct β-scission of other important ions (G) at high temperature.

The propane component is independent of propylene yield and is not produced by hydrogenation of propylene. The propane component is probably produced from propyl carbonium ions produced by β-scission of volatile tertiary carbonium ions without hydrogenation of propylene. For instance, stabilization of (F) ions takes place with lower activation energy of isomerization and thus intramolecular rearrangement to inner tertiary carbon atoms occurs. (F) ions cause intermolecular rearrangement by back biting reactions:

From (G)

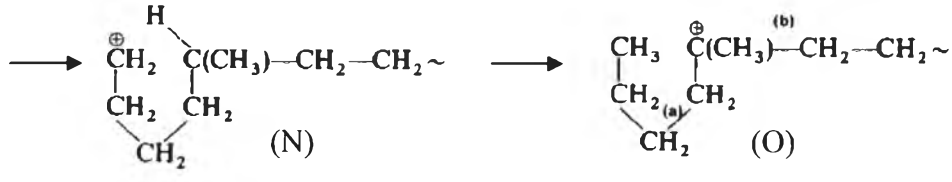

(7)

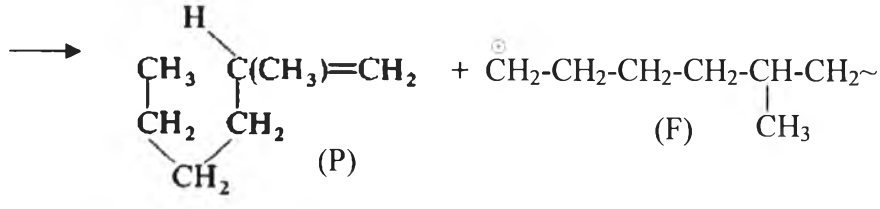

(8)

From (P)

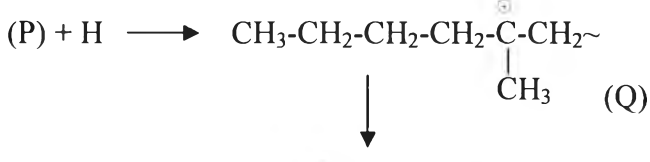

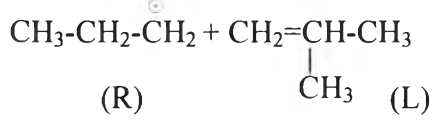

(9)

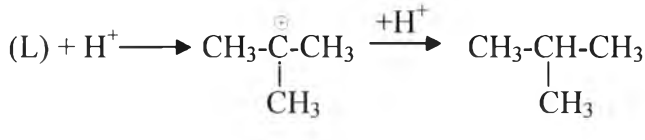

(10)

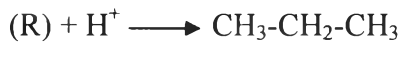

(11)

The stabilization of tertiary carbonium ions (O) proceeds by β-scission at the (b) position to give rise to a more stable fraction (P) than propyl ions ((a) position). Equations (7)-(11) show isobutene and propane are produced. Propane is not produced by the hydrogenation of propylene.

The mechanism of polypropylene is similar to polyethylene but the typical oligomer of polypropylene is 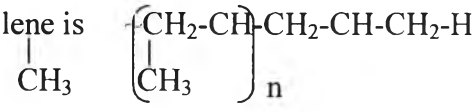

2.5.5. Reactions of Paraffins

Compared to olefins, paraffins have a lower reactivity towards cracking due to a more difficult formation of carbenium ions. Direct formation of a carbenium ion requires the abstraction of a hydride ion. This may proceed at Lewis acid sites or adsorbed carbenium ions can react with paraffins in a bimolecular-type of mechanism. The latter mechanism requires the presence of the adsorbed carbenium ions and can take place if the pore size of the catalyst is large enough to accommodate the necessary transition state (as is the case in zeolite Y and not in ZSM-5).

Indirect formation of carbenium ions is proposed to proceed through the formation of carbonium ions; paraffin reacts with a proton from a Brønsted acid site and the resulting adsorbed carbonium ion is cracked to an adsorbed carbenium ion and hydrogen or a small olefin. The formation of a carbonium ion requires an energetically unfavorable transition state and has high activation energy. This mechanism for activation of paraffins will only be significant in the absence of olefins and is favored by high temperatures, low hydrocarbon partial pressures and low conversions of the paraffins. The occurrence is not expected to be significant when cracking a gasoline mixture that contains olefins. The olefin can easily form carbenium ions and cause cracking of paraffins through the bimolecular cracking mechanisms as discussed above.